# Polygenic signals of sexually antagonistic selection in contemporary human genomes

Filip Ruzicka[1*], Luke Holman[2,3], Tim Connallon[1]

[1] School of Biological Sciences, Monash University, Clayton, Victoria, Australia

[2] School of BioSciences, University of Melbourne, Parkville, Victoria, Australia

[3] School of Applied Sciences, Edinburgh Napier University, Edinburgh, UK

[*]Filip Ruzicka

**Email**: Filip.Ruzicka@monash.edu

**This PDF file includes**:

Main Text

Figures 1 to 5

## Abstract

Mutations that increase fitness in one sex may decrease fitness in the other. Such "sexually antagonistic" (SA) genetic variants can constrain adaptation and increase variability for fitness components (e.g., survival, fertility, and disease susceptibility). However, detecting SA selection in genomes is immensely challenging, as it requires prohibitively large datasets that combine genomic sequences with individual fitness measurements. Here, we use genotypic and reproductive success data from ~250,000 UK Biobank individuals to comprehensively assess the extent of SA genetic variation in humans. We first develop new theoretical models for signals of SA selection spanning a full generational life cycle—including SA polymorphisms affecting survival, reproductive success and overall fitness. Comparing our models with UK Biobank data, we uncover multiple empirical signals of polygenic SA selection, including sex-differential effects of genetic variants on each fitness component, and positive correlations between sex-differential effects and minor allele frequencies. We show that these signals cannot be explained by simple models of sex differences in purifying selection, or by potential confounders such as population structure and sequence mapping errors. We further show that candidate SA sites disproportionately affect functional genomic regions, including polymorphisms associated with quantitative traits and disease. Finally, we examine historical evolutionary processes affecting candidate SA sites, which are consistent with the drift-dominated dynamics predicted by previous theory. Overall, our results support SA genomic variation in humans and highlight its broader functional and evolutionary consequences.

## Introduction

Adaptation of a population to its environment requires heritable genetic variation for fitness [1]. Although many populations show substantial genetic variation for fitness components [2]—including life-history traits such as maturation rate, lifespan, mating success, and fertility [2,3]—genetic trade-offs between components reduce variation for overall fitness, and thereby limit adaptive potential [4]. For example, a mutation that increases the probability of survival to adulthood might simultaneously decrease adult reproductive success (*e.g.*, [5]), weakening the mutation's net fitness effect [4]. In addition to slowing adaptation [6–8], genetic trade-offs can increase standing genetic variation [2,9], give rise to balancing selection [10,11], and favour evolutionary transitions between mating systems [12,13], modes of sex determination [14] and genome structures [15–18].

Sexually antagonistic (SA) genetic polymorphisms—in which the alleles that benefit one sex are harmful to the other—are a type of genetic trade-off that may be common in sexually reproducing species [19]. Theory shows that SA polymorphisms are likely to arise when mutations differentially affect trait expression in each sex, or when mutations similarly affect traits under divergent directional selection between the sexes [20]. Empirical quantitative genetic studies imply that both conditions are frequently met [21–24] and, accordingly, that SA polymorphisms contribute to phenotypic variation in a range of plant and animal populations (*e.g.* [25–27]), including humans [28–30].

Although there is now abundant evidence that SA polymorphisms contribute to phenotypic variation, efforts to identify and characterise SA alleles in genomic data face two formidable challenges [31]. First, methods using explicit fitness measurements to identify SA polymorphisms (*e.g.*, genome-wide association studies (GWAS) of fitness [32]) are rarely feasible, because it is challenging to obtain fitness measurements for large numbers of genotyped individuals under natural conditions [2]. Second, methods using allele frequency

differences between adult females and males as genomic signals of SA viability selection (*e.g.*, between-sex $F_{ST}$ estimates [31,33–40]) are limited in several ways: they have low power to detect individual SA loci, they cannot distinguish SA selection from sex differences in the strength of selection, they are susceptible to artefacts generated by population structure and erroneous mapping of sequence reads to sex chromosomes [31,38,39,41], and they neglect fitness components other than viability, such as reproductive success [31,42]. Previous studies of human genomic data [33,34,41] have, to varying degrees, been affected by each of these issues [31,39,40,42], such that we currently lack robust evidence of SA genomic variation in humans. More generally, these impediments help to explain the limited catalogue of confirmed SA polymorphisms across species [43–45], which currently comprises a handful of loci with exceptionally large phenotypic effects (*e.g.* [46–50]).

Despite these challenges, new datasets and analytical approaches provide opportunities to identify robust genomic signals of SA selection. First, massive 'biobank' datasets, which are widely used in human genomics, sometimes include both genotype and offspring number data [29,51] that can be used to detect loci with SA effects on reproductive components of fitness [31]. Second, estimates of allele frequency differences between sexes—though ill-suited for confidently identifying individual SA loci affecting viability—may nevertheless be amenable to genome-wide tests for *polygenic* SA viability selection [31,33]. Third, polygenic metrics of sex-differential selection (*e.g.*, between-sex $F_{ST}$) may include an appreciable proportion of genuine SA loci in the upper tails of their distributions, providing a set of candidate loci that can collectively yield insights into the general properties of SA polymorphisms (*e.g.*, their functional characteristics and evolutionary dynamics), despite uncertainty about individual candidates.

Here, we extend [31,33] and develop new statistical tests to detect polygenic signals of SA polymorphism affecting viability, reproduction, and total fitness during a full generational

90 cycle. We apply them to the UK Biobank [51], a dataset comprising quality-filtered genotype and
91 offspring number data for ~250,000 men and women. The tests, which are based on between-
92 sex $F_{ST}$ metrics and the covariance between $F_{ST}$ metrics and minor allele frequencies (MAF),
93 reveal polygenic signals of SA selection. Specifically: (*i*) $F_{ST}$ estimates are consistently higher
94 than expected under a null hypothesis in which sex-differential selection is absent; (*ii*) $F_{ST}$
95 estimates are positively correlated with MAF across loci, as predicted under SA selection. We
96 support the $F_{ST}$-based results by: (*i*) replicating these analyses using mixed-model association
97 tests that explicitly control for any systematic differences in the genetic ancestry of female and
98 male individuals; and (*ii*) showing that loci exhibiting artefactual signatures of SA selection
99 due to sequence mapping errors [41] do not occur in our quality-filtered dataset. We further show
100 that candidate SA polymorphisms are preferentially situated in coding and regulatory
101 sequences, and contribute to variation in a range of morphological, behavioural and medically
102 relevant phenotypes. Finally, we use genetic diversity data from global human populations to
103 test for long-term balancing selection, which has been hypothesised to affect SA
104 polymorphisms [10].
105

106 ## Results

107 **Genomic signals of sex differences in selection: theoretical predictions**

108 To illustrate our analytical approach, consider a large, well-mixed population containing many
109 polymorphic, bi-allelic, autosomal loci. At the start of a generation (*i.e.*, at fertilisation),
110 Mendelian inheritance equalises allele frequencies between the sexes (Fig. 1, left box). Loci
111 with sex-differential effects on zygote-to-adult survival will accumulate between-sex allele
112 frequency differences that become apparent among adults (*e.g.*, the black allele becomes
113 enriched in adult males and deficient in adult females because it improves zygote-to-adult
114 survival in males but reduces it in females; Fig. 1, middle box). Furthermore, loci with sex-

115 differential effects on the number of offspring produced will have different transmission rates
116 to the next generation from surviving females *versus* surviving males (*e.g.*, the black allele
117 increases transmission to offspring of males but decreases transmission to offspring of females;
118 Fig. 1, right box). Thus, provided allele frequency and offspring number data are available for
119 adult females and males, we can, in principle, estimate sex-differential effects of genetic
120 variation during a full generational life cycle (Fig. 1), even though allele frequencies among
121 zygotes and gametes are inferred and not directly observed.

122 The UK Biobank provides this opportunity, as it includes genotypes and reported
123 offspring numbers (hereafter "lifetime reproductive success" or LRS, following standard
124 evolutionary biology terminology [29]) among putatively post-reproductive adults (ages 45-69
125 after filtering; see Methods). For a focal autosomal locus with alleles $A_1$ and $A_2$, we denote $\hat{p}_f$
126 and $\hat{p}_m$ ($\hat{q}_f$ and $\hat{q}_m$) the respective estimated frequencies of the $A_1$ ($A_2$) allele in adult females
127 and males of the UK Biobank. Using LRS data of UK Biobank individuals, projected paternal
128 and maternal transmission rates of each allele are estimated as:

$$\hat{p}'_m = \frac{M_{11} + \frac{1}{2}M_{12}}{M_{11} + M_{12} + M_{22}} \quad [1],$$

$$\hat{p}'_f = \frac{F_{11} + \frac{1}{2}F_{12}}{F_{11} + F_{12} + F_{22}}$$

129 where $M_{ij}$ and $F_{ij}$ represent the cumulative LRS of individuals (males and females, respectively)
130 with genotype *ij* (*e.g.*, $M_{11}$, $M_{12}$ and $M_{22}$ correspond to genotypes $A_1A_1$, $A_1A_2$, and $A_2A_2$).

131 Using $F_{ST}$ [52], we partition between-sex allele frequency differentiation over one
132 generation into the differentiation due to: 1) sex-differential variation in survival to adulthood
133 (hereafter "adult $F_{ST}$"; see [31,33,42]); 2) sex-differential variation in adult LRS (hereafter
134 "reproductive $F_{ST}$"); and 3) sex-differential variation in overall fitness (hereafter "gametic

135 $F_{ST}$"). Single-locus estimates of adult $F_{ST}$, reproductive $F_{ST}$ and gametic $F_{ST}$ are defined,
136 respectively, as:

$$\hat{F}_{ST} = \frac{\left(\hat{p}_f - \hat{p}_m\right)^2}{4\bar{p}(1-\bar{p})} \quad [2a],$$

$$\hat{F}_{ST} = \frac{\left(\left(\hat{p}'_f - \hat{p}_f\right) - \left(\hat{p}'_m - \hat{p}_m\right)\right)^2}{4\bar{p}(1-\bar{p})} \quad [2b],$$

$$\hat{F}_{ST} = \frac{\left(\hat{p}'_f - \hat{p}'_m\right)^2}{4\bar{p}'(1-\bar{p}')} \quad [2c],$$

137 where $\bar{p} = \left(\hat{p}_f + \hat{p}_m\right)/2$ and $\bar{p}' = \left(\hat{p}'_f + \hat{p}'_m\right)/2$.

138 In the absence of sex differences in selection (*e.g.*, under neutrality, or under sexually
139 concordant selection of equal magnitude and direction in each sex), with large sample sizes,
140 and excluding single-nucleotide polymorphisms (SNPs) with very low minor allele frequencies
141 (*i.e.*, MAF < 1% in the UK Biobank), we show that adult, reproductive and gametic $\hat{F}_{ST}$
142 converge, respectively, to the following simple null distributions (*SI Appendix*, Section A):

$$\hat{F}_{ST} \approx \left[1/8N_f + 1/8N_m\right]X \quad [3a],$$

$$\hat{F}_{ST} \approx \left[\left(\sigma_f^2/\mu_f^2\right)/8N_f + \left(\sigma_m^2/\mu_m^2\right)/8N_m\right]X \quad [3b],$$

$$\hat{F}_{ST} \approx \left[\left(1 + \sigma_f^2/\mu_f^2\right)/8N_f + \left(1 + \sigma_m^2/\mu_m^2\right)/8N_m\right]X \quad [3c].$$

143 where $X$ is a chi-square random variable with one degree of freedom, $N_f$ and $N_m$ denote adult
144 female and male sample sizes, $\mu_f$ and $\mu_m$ denote mean LRS, and $\sigma_f^2$ and $\sigma_m^2$ denote the
145 corresponding variances in LRS for sampled adult females and males. All three null
146 distributions are independent of MAF, provided sites with very low MAFs are first removed.

147 Relative to the null distributions in eqs. [3a-c], sex differences in selection alter the
148 distributions of each $F_{ST}$ metric in two important ways. First, sex differences in selection inflate
149 $\hat{F}_{ST}$ metrics relative to null model predictions (*SI Appendix*, Section B). These inflations may
150 arise due to polymorphisms under sex-differential selection *and* neutral polymorphisms that

151 hitchhike with selected polymorphisms, but linkage disequilibrium (LD) alone cannot inflate
152 genome-wide $\hat{F}_{ST}$ in the absence of genuine selected polymorphisms (*SI Appendix*, Section C).
153 Thus, $\hat{F}_{ST}$ inflations represent reliable signals of sex-differentially selected polymorphism [31] (if
154 not of the number of independent selected loci), provided population structure and technical
155 artefacts are also controlled (as shown below).

156 Second, sex differences in selection generate statistical associations between $\hat{F}_{ST}$ and
157 MAF that are indicative of the form of sex-differential selection. Specifically, SA selection can
158 generate a positive covariance between each $\hat{F}_{ST}$ metric and MAF, whereas sexually concordant
159 (and/or sex-limited) selection generates a negative covariance (*SI Appendix*, Section B). The
160 negative covariance under sexually concordant selection arises because purifying selection
161 disproportionately lowers the frequency of large-effect alleles relative to small-effect alleles,
162 which is a general feature of loci evolving under purifying selection (see [53]). In contrast, a
163 positive covariance can arise under SA selection because large-effect SA alleles reach
164 intermediate frequencies more easily under balancing selection than small-effect SA alleles,
165 and because intermediate-frequency alleles inflate $\hat{F}_{ST}$ more than low-frequency alleles
166 (irrespective of the strength of balancing selection; *e.g.*, even under drift). Thus, while any sex
167 difference in selection can elevate genome-wide $\hat{F}_{ST}$, positive associations between $\hat{F}_{ST}$ and
168 MAF cannot arise under sex differences in purifying selection alone—instead, they indicate
169 the presence of SA variation. These predictions apply when current patterns of sex-differential
170 selection (which affect measures of $F_{ST}$) are similar to historical patterns of selection (which
171 influence MAF), and are valid under both deterministic and non-deterministic scenarios (*SI*
172 *Appendix*, Section B). Below, we test for both predicted signals of SA selection in the UK
173 Biobank dataset.

174

175 **UK Biobank SNP data**

176 The sample size after removing individuals with close relatedness or non-White British
177 ancestry (see Methods) was $N$ = 250,297 ($N_m$ = 116,661 males and $N_f$ = 133,636 females). We
178 removed rare polymorphic sites (MAF < 1%), sites with low genotype or imputation quality,
179 and sites potentially driving artefactually high between-sex allele frequency differences based
180 on criteria identified by Kasimatis et al. [41]. These criteria were based on differences in missing
181 rates between sexes, deficits of minor allele homozygotes, and excess heterozygosity (*i.e.*,
182 beyond what can be plausibly be explained by sex differences in selection; see *SI Appendix*,
183 Section D). Unless noted, we focus on quality-filtered genotyped SNPs (N = 544,635) in the
184 main text. Results from LD-pruned genotyped SNPs and imputed SNPs (N = 7,844,649)
185 closely match genotyped data and are presented in the *SI Appendix* (Sections E-H), along with
186 full statistical tables.
187
188 **Polygenic signals of sex differences in selection in genome-wide $\hat{F}_{ST}$ distributions**
189 We tested for sex differences in selection by calculating adult $\hat{F}_{ST}$, reproductive $\hat{F}_{ST}$ and
190 gametic $\hat{F}_{ST}$ (eqs. [2a-c]) in the UK Biobank, and contrasting these standardised estimates of
191 allele frequency differentiation between sexes against: (*i*) their respective theoretical null
192 distributions (eqs. [3a-c]), and (*ii*) empirical null distributions generated by a single random
193 permutation of male and female labels among individuals or, in the case of reproductive $\hat{F}_{ST}$, a
194 single permutation of LRS among individuals of a given sex (see Methods).
195 All three $\hat{F}_{ST}$ metrics showed significantly greater differentiation than predicted by their
196 theoretical and empirical null distributions, consistent with sex differences in selection
197 contributing to genome-wide allele frequency differentiation between the sexes. Mean adult
198 $\hat{F}_{ST}$ in the observed data was larger than predicted by both null distributions (theoretical null:
199 $2.012\times10^{-6}$; permuted null: $2.014\times10^{-6}$; observed: $2.107\times10^{-6}$; Wilcoxon and Kolmogorov-
200 Smirnov tests, $p<0.001$; Fig. 2A,D; *SI Appendix*, Section E, Figs. S1-5; Tab. S1), with a 20.4%

excess of SNPs in the top 1% quantile of the theoretical null and a 16.5% excess in the top 1% quantile of the empirical null ($\chi^2$ tests, p<0.001). Mean reproductive $\hat{F}_{ST}$ was larger than predicted by both nulls (theoretical: $8.667\times10^{-7}$; permuted: $8.770\times10^{-7}$; observed: $9.049\times10^{-7}$; Wilcoxon and Kolmogorov-Smirnov tests, p<0.001; Fig. 2B,E; *SI Appendix*, Section E, Figs. S1-5; Tab. S1), with a 17.9% excess of SNPs in the top 1% quantile of the theoretical null and a 11.5% excess in the top 1% quantile of the empirical null ($\chi^2$ tests, p<0.001). Mean gametic $\hat{F}_{ST}$ was larger than predicted by both nulls (theoretical: $2.874\times10^{-6}$; permuted: $2.874\times10^{-6}$; observed: $2.986\times10^{-6}$; Wilcoxon and Kolmogorov-Smirnov tests, p<0.001; Fig. 2C,F; *SI Appendix*, Section E, Figs. S1-5; Tab. S1), with a 17.1% excess of SNPs in the top 1% of the theoretical and empirical nulls ($\chi^2$ tests, p<0.001).

Signals of sex differences in selection in adult, reproductive, and gametic $\hat{F}_{ST}$ were polygenic: although each $\hat{F}_{ST}$ metric was markedly inflated on a genome-wide scale, no individual locus reached a p-value below the Bonferroni-corrected threshold ($9.181\times10^{-8}$; *SI Appendix*, Section E, Figs. S6-7). For example, the minimum p-values were $3.260\times10^{-7}$ for adult $\hat{F}_{ST}$ (minimum q-value=0.101), $7.036\times10^{-7}$ for reproductive $\hat{F}_{ST}$ (minimum q-value=0.383), and $2.858\times10^{-6}$ for gametic $\hat{F}_{ST}$ (minimum q-value=0.346).

**Positive associations between $\hat{F}_{ST}$ and MAF indicate SA selection**

To distinguish polygenic signals of SA selection from other modes of selection that might also give rise to elevated $\hat{F}_{ST}$ (*e.g.*, selection acting only on one sex, or differences in the strength but not the direction of selection between sexes), we examined the association between MAF and each $\hat{F}_{ST}$ metric. This association can be positive under SA selection but should be negative under sex-differential purifying selection, provided patterns of sex-differential selection are relatively consistent over time (see above). Consistent with SA selection, we observed positive correlations between MAF and all three $\hat{F}_{ST}$ metrics (adult $\hat{F}_{ST}$, $\rho$=0.014, p<0.001; reproductive

226 $\hat{F}_{ST}$, $\rho$=0.010, p<0.001; gametic $\hat{F}_{ST}$, $\rho$=0.010, p<0.001; Fig. 3A-C; *SI Appendix*, Section F,
227 Figs. S9-13; Tab. S2), with all correlations stronger in observed than null data (*SI Appendix*,
228 Section F, Fig. 3D-F; Figs. S10,12).
229
230 **Signals of SA selection persist after controlling for sex-specific population structure**
231 In principle, genome-wide elevations in $\hat{F}_{ST}$ can arise entirely from systematic differences in
232 ancestry (population structure) between sexes and in the absence of genuine sex differences in
233 selection [31,42]. We therefore replicated our analyses using mixed-model association tests that
234 are analogous to $\hat{F}_{ST}$ but which explicitly correct for population structure.
235 We first evaluated signals of sex differences in viability selection by performing a
236 GWAS of sex [31,41,54] using standardised estimates of the log-odds ratio ($\hat{\mathcal{L}}_{ST}$; see Methods). $\hat{\mathcal{L}}_{ST}$
237 quantifies between-sex allele frequency differences among adults (like adult $\hat{F}_{ST}$) while
238 controlling for population structure by including a kinship matrix of genome-wide relatedness
239 between individuals. As expected, $\hat{\mathcal{L}}_{ST}$ was highly correlated with adult $\hat{F}_{ST}$ (Spearman's
240 $\rho$=0.988; p<0.001; *SI Appendix*, Section E, Fig. S8) and was elevated relative to an empirical
241 null distribution generated through permutation of sex labels (null mean $\hat{\mathcal{L}}_{ST}$: $5.000\times10^{-7}$; mean
242 observed: $5.188\times10^{-7}$; Wilcoxon and Kolmogorov-Smirnov tests, p<0.001; *SI Appendix*,
243 Section E, Figs. S1-5; Tab. S1), with a 14.0% excess of SNPs in the top 1% quantile of the
244 empirical null ($\chi^2$ test, p<0.001), and a significant SNP-heritability of sex
245 ($h^2_{SNP}$±SE=0.014±0.002).
246 We then tested for a signal of sex differences in selection through reproductive fitness
247 components by performing separate GWAS for LRS in females and males (controlled for
248 population structure) and quantifying the difference between female and male effect sizes using
249 a *t*-statistic (|*t*|; see Methods). As expected, the distribution of |*t*| was highly correlated to
250 reproductive $\hat{F}_{ST}$ (Spearman's $\rho$=0.921; p<0.001; *SI Appendix*, Section E, Fig. S8) and was

elevated relative to an empirical null generated by permutation of LRS within each sex (null mean $|t|$=0.797, observed mean $|t|$=0.817, Wilcoxon and Kolmogorov-Smirnov tests, p<0.001; *SI Appendix*, Section E, Figs. S1-5; Tab. S1), with an 17.9% excess of SNPs in the top 1% quantile of the empirical null ($\chi^2$ test, p<0.001). Finally, $\hat{\mathcal{L}}_{ST}$ and $|t|$ were both positively correlated with MAF ($\hat{\mathcal{L}}_{ST}$: $\rho$=0.014, p<0.001; $|t|$: $\rho$=0.010, p<0.001; *SI Appendix*, Section F, Figs. S9-13; Tab. S2), confirming the signals of SA selection detected with $\hat{F}_{ST}$ metrics.

**Functional analyses of candidate SA SNPs**

If loci with high $\hat{F}_{ST}$ (or related metrics) include genuine SA polymorphisms, they should preferentially be found in functionally important regions in the genome, whereas such enrichment is not expected if the observed $\hat{F}_{ST}$ inflation results from random chance, genotyping errors, or sex-specific population structure. We therefore conducted several enrichment tests, both to support our inference that SA selection is occurring and to explore functional effects of candidate SA loci.

First, we asked whether sites with high sex-differentiation were disproportionately situated in "genic" regions, defined broadly to include coding and regulatory elements (see Methods). This test revealed consistently positive associations between each metric of sex-differential selection and genic status (Binomial GLMs: adult $\hat{F}_{ST}$, p=0.021; $\hat{\mathcal{L}}_{ST}$, p=0.018; reproductive $\hat{F}_{ST}$, p=0.0497; $|t|$, p=0.025; gametic $\hat{F}_{ST}$, p=0.026; Fig. 4A-C; *SI Appendix*, Section G, Figs. S14-15; Tab. S3). Polygenic patterns of genic enrichment in the imputed data were similar to the genotyped data (*SI Appendix*, Section G, Fig. S16; Tab. S3), though extremely differentiated loci were less often genic in the imputed data, which may reflect higher genotype uncertainty among imputed sites and the consequently higher likelihood of artefacts.

275 Second, we used summary statistics from the Neale laboratory database of UK Biobank
276 GWAS to explore whether metrics of sex-differential selection were associated with candidate
277 loci for 43 phenotypes, chosen for their medical relevance and/or relationship to phenotypic
278 sex differences. Though few traits were associated after FDR-correction in the genotyped data
279 (*SI Appendix*, Section G, Fig. S17), we found multiple associations in the imputed data, where
280 the number of loci (and thus statistical power) is larger (Fig. 4D). For example, several disease-
281 relevant traits (high blood pressure; red blood cell count; diseases of the musculoskeletal
282 system and connective tissue; heel bone mineral density) and behavioural traits (neuroticism
283 score) were associated with metrics of sex-differential survival and LRS (Mann-Whitney tests;
284 FDR-corrected $p < 0.05$). We also found trait associations that were unique to metrics of sex-
285 differential survival (white blood cell count; body fat percentage) and LRS (standing height;
286 platelet count). Loci affecting testosterone had lower-than-average gametic $\hat{F}_{ST}$.
287
288 **Evolutionary histories of candidate SA SNPs**
289 To gain insights into the evolutionary dynamics of candidate SA sites, we tested for signals of
290 long-term balancing selection, which can, under certain scenarios of selection and dominance,
291 stably maintain SA polymorphisms over long periods of time [10]. We used three metrics of
292 balancing selection: allele age estimates from the Atlas of Variant Age database [55], between-
293 population $\hat{F}_{ST}$ from four worldwide non-European populations from the 1000 Genomes
294 Project [56], and three independent sets of candidate loci for balancing selection [57–59]. In each
295 case, we looked for associations between $\hat{F}_{ST}$ metrics of sex-differential selection and metrics
296 of balancing selection, while controlling for ascertainment bias of intermediate-frequency
297 alleles (which are, on average, older) among highly sex-differentiated sites (*i.e.*, Fig. 3; see
298 Methods). Under long-term balancing selection, we would expect candidate SA alleles (and
299 linked loci) to be older, to exhibit lower between-population $\hat{F}_{ST}$, and to disproportionately co-

300 localise with previous candidates for balancing selection, compared to non-candidate SA sites
301 with similar allele frequencies in the UK Biobank.

302 We found no significant associations between metrics of sex-differential selection and
303 metrics of balancing selection, including allele age (adult $\hat{F}_{ST}$, Spearman's $\rho$=0.001, p=0.353;
304 reproductive $\hat{F}_{ST}$, Spearman's $\rho$=0.000, p=0.919; gametic $\hat{F}_{ST}$: Spearman's $\rho$=0.002, p=0.092;
305 Fig. 5; *SI Appendix*, Section H, Figs. S18,21,22; Tab. S4), between-population $\hat{F}_{ST}$ (*SI*
306 *Appendix*, Section H, Fig. S19; Tab. S5), or previous candidates for balancing selection (*SI*
307 *Appendix*, Section H, Figs. S20,21,23; Tabs. S6-8). Overall, there is no compelling evidence
308 for long-term balancing selection among candidate SA SNPs.

309

## 310 Discussion

311 Sex differences in directional selection on phenotypes have been reported in a wide range of
312 animal taxa [21–23,60], including post-industrial human populations [29,30], yet population genomic
313 signals of SA selection have been extremely difficult to establish. The reason is simple: sexual
314 reproduction equalises autosomal allele frequencies between the sexes every generation, which
315 restricts genetic divergence between males and females and, in effect, precludes the use of tests
316 that are commonly used to detect other forms of selection (*e.g.*, McDonald-Kreitman tests for
317 positive selection and $F_{ST}$ outlier tests for spatially-varying selection [61–63]). Published studies
318 using human genomic data illustrate the challenges of studying SA polymorphisms, including
319 sample sizes that may be insufficient for detecting polygenic signals of selection [31,33,34], lack
320 of controls for population structure or technical artefacts [33,34], and/or absence of data
321 concerning reproductive components of fitness [33,34,41].

322 Here, by developing new metrics of SA genomic variation and applying them to data
323 from a quarter-million UK adults, we present robust evidence for polygenic sex-differential
324 selection in humans. Specifically, UK Biobank individuals showed sex differences in allele

325 frequencies—both among adults and their (projected) offspring—that consistently exceeded
326 expectations defined by our theoretical null models for viability, reproductive and total fitness,
327 and these signals persisted after controlling for sex-specific population structure. Our analyses
328 of reproductive $\hat{F}_{ST}$ and $|t|$ metrics are particularly compelling because they control for allele
329 frequency differences between samples of adults of each sex and rule out factors that might
330 otherwise affect estimated adult allele frequencies in the UK Biobank (*e.g.*, mis-mapping of
331 reads to sex chromosomes, participation bias [54]; see below). These elevations in reproductive
332 $\hat{F}_{ST}$ and $|t|$ are consistent with previous observations in post-industrial human populations,
333 including variation in female and male LRS [64] (a necessary precondition for sex-differential
334 selection), widespread sex differences in the genetic basis of quantitative traits (*e.g.*, in the UK
335 BioBank [65]), and SA selection on phenotypes (*e.g.*, height [29,30] and multivariate trait
336 combinations [64]), which should collectively lead to SA polymorphisms throughout the genome
337 [20]. In particular, our finding that candidate loci for standing height were positively associated
338 with reproductive $\hat{F}_{ST}$ and $|t|$ is in line with earlier reports of SA selection acting on adult height
339 [29,30]. Furthermore, the positive associations we report between MAF and $\hat{F}_{ST}$ (and related
340 metrics) are consistent with SA selection and cannot be explained by simple models of sex
341 differences in purifying selection. Though it is conceivable that contemporary patterns of
342 selection (which influence $\hat{F}_{ST}$) are sufficiently different from historical patterns of selection
343 (which influence MAF) that our models do not reflect the evolutionary causes of the positive
344 associations between MAF and $\hat{F}_{ST}$, SA polymorphisms represent a parsimonious explanation
345 for the positive correlation we detect [29,30].

346 At first glance, the signals of SA viability selection in adult $\hat{F}_{ST}$ and $\hat{\mathcal{L}}_{ST}$ metrics may
347 seem surprising given the low rates of infant and juvenile mortality in post-industrial human
348 populations [64]. However, mortality after fertilisation but before birth is common (on the order
349 of 50% [66]), giving ample opportunity for sex differences in mortality to generate allele

frequency differences [67]. Another possibility, raised by Pirastu et al. [54], is that sex differences in adult allele frequencies arise because of sex differences in the genetic basis of individuals' predisposition to take part in the UK Biobank study, which relies upon active participation. To support this interpretation, they reported significant SNP heritability of sex (a polygenic measure of sex differences in allele frequencies) in biobanks relying on active participation (UK Biobank; 23andMe), and non-significant SNP heritability in biobanks using passive participation (Biobank Japan; Finngen; iPsych). However, this result might instead reflect differences in statistical power, as passive participation studies are considerably smaller than active participation studies. Further work (*e.g.*, parent-offspring trio analyses that control for participation effects [67]; replication studies in other Biobank-scale datasets) will be required to conclusively distinguish the relative contributions of SA selection and participation bias on allele frequency differentiation among male and female adults, and to assess whether SA variants affecting viability tend to increase or decrease LRS within and across sexes.

We also found that candidate SA sites were preferentially found within coding and regulatory elements, and contributed to variation in morphological, physiological, behavioural, and medically relevant phenotypes. These functional analyses provide further evidence that elevated between-sex $\hat{F}_{ST}$ reflects selection rather than technical artefacts. They also lend support to the hypothesis that SA alleles contribute to disease susceptibility [9]. For example, loci associated with bone mineral density and red blood cell count showed elevated signals of SA selection. Bone mineralisation and red blood cell count are sexually dimorphic traits that positively genetically correlate with musculoskeletal disease and high blood pressure [68]. Accordingly, loci associated with musculoskeletal disease and high blood pressure also showed elevated sex-differentiation.

Our analyses do not reveal clear signals of long-term balancing selection among candidate SA sites, which may stem from several factors. First, balancing selection—to the

375 extent that it maintains SA polymorphisms—may be too recent to generate a clear statistical
376 signal in our analyses [69]. Second, balancing selection at SA loci may be *effectively* weak, owing
377 to relatively small $N_e$ in humans [70] and the high susceptibility of SA alleles to genetic drift [71].
378 Third, long-term balancing selection may be present, but statistical tests for it may be too weak
379 to stand out from the background noise of false positives in our metrics and the datasets used
380 to quantify balancing selection [72]. Overall, evidence that SA polymorphisms contribute to
381 standing genetic variation—as in our study—is at present stronger than evidence that they are
382 stably maintained by balancing selection (but see [32]).

383 To what extent should we expect the patterns reported here to replicate across studies?
384 Many taxa exhibit greater variance for reproductive success than humans [73], generating higher
385 potential for polygenic signals of SA selection. In line with this, polygenic inflation of adult
386 $\hat{F}_{ST}$ has previously been documented in modest samples of pipefish and flycatchers [31,36,37],
387 suggesting that sex differences in selection might be stronger in those species than in humans.
388 Yet while polygenic signals of SA selection may replicate across studies, candidate SA
389 polymorphisms may not. One reason is that environmental differences between populations
390 (*e.g.*, cultural differences in family planning between human populations) could alter the set of
391 loci under SA selection. Additionally, the noisiness of polygenic signals of SA selection [31,42],
392 along with the near-certainty that most polymorphic loci have small effects on fitness [74],
393 generates variation in the set of candidate SA polymorphisms *identified* across populations or
394 generations, even if causal SA polymorphisms do not differ. Similar predictions apply to
395 scenarios of polygenic local adaptation with high gene flow [75], whose population genetic
396 dynamics strongly parallel SA selection [31,76].

397 Finally, the extent to which signals of balancing selection will co-occur with SA
398 polymorphisms awaits further study, but given the pronounced sensitivity of SA balancing
399 selection to genetic drift [71,77], we should expect the relationship between signals of SA selection

400 and balancing selection to vary with $N_e$. For example, previous work in *Drosophila*
401 *melanogaster* indicates that candidate SA polymorphisms segregate across worldwide
402 populations and even species [32], and in contrast to the results of our study, these candidates are
403 putatively maintained under balancing selection. A parsimonious explanation for these
404 contrasting findings is that the effectiveness of balancing selection is lower in humans than
405 fruit flies due to much smaller $N_e$.
406

407 # Methods

408 **Quality control of UK Biobank data**

409 Access to UK Biobank data was granted under project number 52049. We used sample-level
410 information provided by the UK Biobank (see [51] for details) to perform individual-level
411 (phenotypic) quality controls. Specifically, we excluded individuals with high relatedness (3rd
412 degree or closer), non-White British ancestry, high heterozygosity and high missing rates.
413 Individuals whose reported sex did not match their inferred genetic sex, whose age was less
414 than 45 years, and aneuploids were also excluded. In addition to site-level quality-controls
415 implemented by the UK Biobank [51], we used PLINK and PLINK2 [78] to remove sites that were
416 non-diallelic, had MAF<1%, missing rates>5%, and p-values<$10^{-6}$ in tests of Hardy-Weinberg
417 equilibrium. These filters were applied to all autosomal genotyped and imputed sites. We
418 further removed imputed sites with INFO score ≤0.8, denoting poor imputation.
419

420 **Artefact filtering in UK Biobank data**

421 Mis-mapping of autosomal reads to sex chromosomes can generate between-sex allele
422 frequency differences in the absence of sex differences in selection [31,41] (though note that such
423 artefacts are not expected to inflate metrics of adult reproductive success, since these metrics
424 control for any sex differences in allele frequencies among adults). To remove mis-mapping

425 artefacts, we excluded: (*i*) sites with heterozygosity levels that exceeded what could plausibly
426 be expected under SA selection (see below and *SI Appendix*, Section D); (*ii*) sites with a deficit
427 of minor allele homozygotes; (*iii*) sites exhibiting large differences in missing rate between
428 sexes. These three patterns have previously been shown to associate with mis-mapping of reads
429 to sex chromosomes [41].

430 To remove sites with artificially inflated heterozygosity, we estimated $F_{IS}$ for each SNP,
431 defined as:

432 $$\hat{F}_{IS} = \frac{P_{Aa}}{2\bar{p}(1-\bar{p})} - 1$$

433 where $P_{Aa}$ denotes the frequency of heterozygotes for a given locus and $\bar{p}$ the sex-averaged
434 allele frequency. For a SA locus at polymorphic equilibrium, the distribution of $\hat{F}_{IS}$ is well
435 approximated by a normal distribution with expectation and variance as follows:

436 $$\mathrm{E}\left[\hat{F}_{IS}\right] \approx \frac{1}{2n} + \frac{p(1-p)}{4}\left(\frac{s_{\max}}{1-ps_{\max}}\right)^2$$

437 $$\mathrm{var}\left[\hat{F}_{IS}\right] = \frac{1}{n}$$

438 where $n$ is total sample size of adults, $p$ the minor allele frequency, and $s_{\max} = \max(s_m, s_f)$ with
439 $s_m$ and $s_f$ representing male and female selection coefficients (*SI Appendix*, Section D). To
440 identify SNPs with excess heterozygosity, we compared $\hat{F}_{IS}$ in the observed data to expected
441 $\hat{F}_{IS}$ under strong SA selection ($s_{\max}$=0.2) by performing a one-tailed Z-test for excess
442 heterozygosity. We thus obtained p-values for each locus, corrected p-values for multiple
443 testing using Benjamini-Hochberg false discovery rates [79], and removed sites with FDR q-
444 values below 0.05. Note that this test was designed to eliminate mapping errors, but it will also
445 eliminate sites under strong (but not weak or moderately strong) sex-differential selection. The
446 net effect of applying this filter is a slightly conservative test of sex-differential selection.

447 To identify sites with a deficit of minor allele homozygotes, we compared the observed
448 frequency of minor allele homozygotes to the expected frequency under Hardy-Weinberg
449 equilibrium ($p^2$, where $p$ is the frequency of the minor allele) by performing a one-tailed
450 binomial test, removing sites with FDR q-values below 0.05. Tests for excess heterozygosity
451 and deficits of minor allele homozygotes were performed across all individuals (regardless of
452 sex), and also for each sex separately. Sites were removed if they exhibited q-values below
453 0.05 in any of the three tests (*i.e.*, both sexes combined, females, and males). Finally, to assess
454 differences in missing rate between the sexes, we performed a $\chi^2$ test, removing sites with
455 FDR q-values below 0.05.

456 Reassuringly, applying these filters eliminated all 8 sites that Kasimatis et al. [41]
457 identified as false-positives for SA viability selection in the genotyped data. One remaining
458 site (rs114928327) appeared in the imputed data but exhibited lower-than-average adult $\hat{F}_{ST}$
459 and $\hat{\mathcal{L}}_{ST}$.

460

461 **Quantifying polygenic signals of sex differences in selection**

462 *$\hat{F}_{ST}$-based metrics*

463 Allele frequencies in adults of each sex were obtained directly from sequence data and used to
464 calculate adult $\hat{F}_{ST}$ for each polymorphic site (post-filtering). Allele frequency differences
465 between sexes were estimated using the $\hat{F}_{ST}$ metrics presented in eqs. [2a-c]. Data on offspring
466 number were obtained from field 2405 "Number of children fathered", for males, and field
467 2734 "Number of live births", for females (hereafter "lifetime reproductive success" (LRS)).
468 Because some individuals were asked to report offspring number at repeated assessment points,
469 we considered the maximum offspring number reported as the definitive value of LRS for that
470 individual. Though mis-estimation of LRS for each individual cannot be definitively excluded
471 (*e.g.*, due to mis-reporting, or additional reproduction after data collection), we minimised this

472 possibility by removing individuals: (*i*) younger than 45 years of age (see "Quality control of
473 UK Biobank data"); (*ii*) reporting fewer offspring at a later assessment point than at an earlier
474 assessment point; (*iii*) with 20 or more reported offspring numbers (large offspring numbers
475 often ended in zero—*e.g.,* 20, 30, 50, 100—and were thus considered less reliable).
476 Furthermore, we note that uncounted LRS data adds imprecision but should not systematically
477 bias our analyses. Finally, previous research indicates that offspring number represents a good
478 proxies for LRS in post-industrial human populations, based on observations of positive
479 genetic correlations between offspring and grand-offspring numbers across generations [80].

480 The theoretical null distributions presented in eqs. [3a-c] apply to genome-wide data in
481 which the sample of female and male sequences are constant across loci. For each null, we
482 adjusted for locus-specific missing data (which causes variation in locus-specific sample sizes)
483 by allowing sample sizes to vary across loci (*i.e.*, $N_{f_i}$ and $N_{m_i}$ adults, or $2N_{f_i}$ and $2N_{m_i}$
484 sequences, per diploid locus *i*).

485

486 *Case-control GWAS of sex*

487 To complement the test for sex-differential viability selection based on adult $\hat{F}_{ST}$, we performed
488 a GWAS of sex [31,41,54]. By analogy to adult $\hat{F}_{ST}$, loci with sex-differential effects on viability
489 in a GWAS of sex will tend to have relatively large absolute log-odds ratios (corresponding to
490 relatively large allele frequency differences between sexes). Unlike adult $\hat{F}_{ST}$, this approach
491 additionally permits the inclusion of covariates in the GWAS to account for population
492 structure and other possible confounders [31].

493 We used BOLT-LMM to run a mixed-model GWAS [81], using a kinship matrix to
494 account for population structure. The kinship matrix was constructed from a subset of 241,669
495 LD-pruned genotyped SNPs (settings '--indep-pairwise 50 10 0.2' in PLINK; MAF>0.01). We
496 added individual age (field 54) and assessment centre (field 21003) as fixed-effect covariates.

497 To facilitate comparisons with adult $\hat{F}_{ST}$, we standardised the regression coefficients (log-odds
498 ratios) from the GWAS by allele frequency, such that:

499 $$\hat{\mathcal{L}}_{ST} = (\sqrt{\bar{p}(1-\bar{p})}\hat{\mathcal{L}})^2$$

500 where $\hat{\mathcal{L}}$ is the log-odds ratio and $\bar{p}$ is the sex-averaged allele frequency among adults. We also
501 quantified a genome-wide signal of sex-differential viability selection by estimating the SNP-
502 heritability of sex, in BOLT-LMM.

503

504 *t-statistic for sex differences in GWAS of LRS*

505 To complement the test for sex differences in selection on LRS based on reproductive $\hat{F}_{ST}$, we
506 performed a GWAS of LRS in each sex separately, using a mixed-model GWAS implemented
507 in BOLT-LMM, which allowed us to correct for population structure in effect size estimates.
508 Following [82], we quantified differences in male and female effect size estimates by means of a
509 *t*-statistic, defined as:

510 $$|t| = \left|\frac{\beta_M - \beta_F}{\sqrt{SE_M^2 + SE_F^2 - 2\rho SE_M SE_F}}\right|$$

511 where $\beta_M$ and $\beta_F$ are estimated effect sizes obtained from sex-stratified
512 GWAS, $SE_M$ and $SE_F$ are sex-specific standard errors, and $\rho$ is the between-sex rank
513 correlation among genome-wide LD-pruned loci. Loci with elevated values of $|t|$ in observed
514 relative to permuted data denote candidate loci with sex-differential effects on LRS.

515

516 *Statistical comparisons of null and observed distributions*

517 Null distributions for each metric of sex differences in selection (*i.e.*, adult $\hat{F}_{ST}$, $\hat{\mathcal{L}}_{ST}$,
518 reproductive $\hat{F}_{ST}$, $|t|$, and gametic $\hat{F}_{ST}$) have been theoretically derived (for the $\hat{F}_{ST}$ metrics; see
519 *SI Appendix*, Section A) and/or obtained empirically through permutation (all five metrics).
520 Empirical null distributions were generated as follows. For adult $\hat{F}_{ST}$, gametic $\hat{F}_{ST}$ and $\hat{\mathcal{L}}_{ST}$, we

521 performed a single permutation of female and male labels and re-calculated the statistic in the
522 permuted data. For reproductive $\hat{F}_{ST}$ and $|t|$, we performed a single permutation of LRS values
523 within each sex—without permuting sex—and re-calculated the statistic in the permuted data.
524 Permuting LRS without permuting sex allows allele frequencies to differ between sexes (as
525 would happen if, for example, sex-differential viability selection is occurring among juveniles)
526 while randomising effects of genotype on LRS (which ensures that sex-differential selection
527 on LRS cannot contribute to the empirical null). Performing a single permutation for each
528 metric was sufficient for our purposes because we were focussed on testing a cumulative signal
529 of selection across loci, rather than establishing statistical significance at the single-locus level.
530 To test for elevations of each metric relative to the (theoretical or empirical) nulls, we
531 performed Wilcoxon Rank-Sum and Kolmogorov-Smirnov tests. These tests assess differences
532 in the median and distribution of the observed and null data, respectively. As a complementary
533 way of comparing observed and null data, we quantified enrichment of observed values in the
534 top 1% of each null using a $\chi^2$ test. Finally, we estimated the difference between the mean
535 value of the metric in the observed data and the mean value of the metric in each null, obtaining
536 95% confidence intervals and empirical p-values through bootstrapping (1,000 replicates;
537 where each replicate consists of the set of relevant genotyped or imputed SNPs, sampled with
538 replacement).
539
540 **Associations between metrics of sex differences in selection and MAF**
541 To test for associations between metrics of sex differences in selection and MAF, we performed
542 a Spearman's rank correlation between each metric and MAF. We also tested whether the
543 relationship between metrics of sex differences in selection and MAF was more pronounced in
544 the observed data than in the (theoretical or empirical) nulls by estimating the difference
545 between correlations in the observed data and correlations in the null data among 1,000

546 bootstrap replicates (as above), thereby generating 95% confidence intervals and empirical p-
547 values.
548
549 **Functional analyses**
550 Following research on candidate locally adapted loci [83–85], we tested whether loci exhibiting
551 elevated values of each metric of sex-differential selection were disproportionately situated in
552 putatively functional regions of the genome. We categorised SNPs as either intergenic or non-
553 intergenic based on annotations obtained with SnpEff [86]. We then fitted a logistic regression
554 model to our data, with annotation (genic/intergenic) as the binary response variable and the
555 metric of sex differences in selection under consideration as an independent variable. We also
556 examined whether associations between metrics of sex differences in selection and genic status
557 were more pronounced in the observed data than under (theoretical or empirical) nulls by
558 calculating the difference between the regression coefficients in the observed and null data
559 among 1,000 bootstrap replicates (as above).
560 We compared our five metrics to previously-documented GWAS hits from Neale
561 laboratory's analyses of all UK Biobank traits [68]. Briefly, we compared the average value of
562 the focal metric (*e.g.*, adult $\hat{F}_{ST}$ or $|t|$) between loci that were and were not associated ($\alpha = 10^{-}$
563 $^{4}$) with the focal phenotype (n = 43 traits) using a Mann-Whitney test, and then FDR-corrected
564 the resulting p-values. These analyses were performed on LD-pruned SNPs to reduce pseudo-
565 replication due to LD between loci. Analyses are fully documented (including code and results)
566 at https://lukeholman.github.io/ukbb_sex_fst.
567
568 **Quantifying signals of long-term balancing selection**
569 *Allele ages*

570 If candidate SA variants experience sufficiently strong and sustained balancing selection
571 relative to the countervailing effects of genetic drift, we expect them to be older than the
572 genome-wide average [69]. We used the Atlas of Variant Age database to obtain allele age
573 estimates for genome-wide variants [55]. Estimates of allele age in this database apply to the non-
574 reference (*i.e.*, alternative) allele and are derived from coalescent modelling of the time to the
575 most recent common ancestor using the "Genealogical Estimation of Variant Age" method (see
576 [55] for details). Estimates of allele age make use of genomic data from: (*i*) the 1000 Genomes
577 Project; (*ii*) the Simons Genome Diversity Project; (*iii*) both datasets combined. For each site
578 in the UK Biobank, we obtained the median estimate of allele age from the combined dataset
579 (when available), from the 1000 Genomes Project, or the Simons Genome Diversity Project
580 (when neither alternative estimate was available).
581
582 *Between-population $F_{ST}$*
583 If candidate SA variants experience sufficiently strong balancing selection maintaining a fixed
584 polymorphic equilibrium, they should exhibit lower-than-average allele frequency differences
585 *between* populations [69]. We obtained allele frequency data from four non-European populations
586 from the 1000 Genomes Project: Southern Han Chinese (CHS, N=105); Yoruba Nigerians
587 (YRI, N=108); Puerto Ricans (PUR, N=104) and Gujarati Indians (GIH, N=103). For each
588 pairwise combination of populations, we estimated between-population $\hat{F}_{ST}$, as:

589 $$\hat{F}_{ST} = \frac{(\hat{p}_1 - \hat{p}_2)^2}{4\bar{p}(1-\bar{p})}$$

590 where $\hat{p}_1$ and $\hat{p}_2$ are allele frequency estimates in the relevant pair of populations, and $\bar{p} =$
591 $(\hat{p}_1 + \hat{p}_2)/2$.
592
593 *Previous candidates for balancing selection*

594 If candidate SA variants experience strong balancing selection, they should disproportionately
595 co-occur with previously identified candidates for balancing selection. We used three
596 independent sets of candidate sites for balancing selection to investigate this possibility [57–59]:
597 (*i*) the dataset of Andrés et al. [57], which consists of 64 genes exhibiting elevated polymorphism
598 (as determined using the Hudson-Kreitman-Aguadé test) and/or intermediate-frequency alleles
599 across 19 African-American or 20 European-American individuals; (*ii*) the dataset of
600 DeGiorgio et al. [59], which consists of 400 candidate genes exhibiting elevated $T_1$ or $T_2$ statistics
601 among 9 European (CEU) and 9 African (YRI) individuals. $T_1$ or $T_2$ statistics quantify the
602 likelihood that a genomic region exhibits levels of neutral polymorphism that are consistent
603 with a linked balanced polymorphism; (*iii*) the dataset of Bitarello et al. [58], which consists of
604 1859 candidate genes exhibiting elevated values of "Non-Central Deviation" (NCD) statistics.
605 NCD statistics also quantify the likelihood that given genomic regions are situated nearby a
606 balanced polymorphism, using polymorphism data from 50 random individuals from two
607 African (YRI; LWK) and European (GBR; TSI) populations and divergence data from a
608 chimpanzee outgroup.
609 We assigned each site in the UK Biobank dataset to a gene using SnpEff [86] and
610 categorised sites as candidates or non-candidates for balancing selection based on whether they
611 were annotated as belonging to a candidate or non-candidate in each of the three
612 aforementioned datasets.
613
614 *Statistical associations between metrics of sex-differential selection and balancing selection*
615 To test whether signals of sex differences in selection were associated with signals of balancing
616 selection, we performed Spearman's rank correlations between alternative allele age (scaled
617 by alternative allele frequency in the UK Biobank, to control for ascertainment bias) and each
618 metric of sex differences in selection. For between-population $\hat{F}_{ST}$, we performed multiple

linear regressions, with metric of sex differences in selection as the independent variable and MAF in the UK Biobank as a fixed-effect covariate (to control for ascertainment bias). For previous candidates for balancing selection, we performed multiple logistic regressions, where candidate/non-candidate status was treated as a binary response variable, metric of sex differences in selection as the independent variable, and UK Biobank MAF as a fixed-effect covariate. We also tested whether associations between metrics of balancing selection and sex differences in selection were more pronounced in the observed data than under (theoretical or empirical) null. This was done by calculating the difference between the summary statistics (*i.e.*, correlation or regression coefficients, as outlined above) in the observed and null data among 1,000 bootstrap replicates.

632 **References**


633 1. Fisher, R. A. *The Genetical Theory of Natural Selection*. *Genetics* (Clarendon Press,
634 1930). doi:10.1038/158453a0.
635 2. Charlesworth, B. Causes of natural variation in fitness: evidence from studies of
636 *Drosophila* populations. *Proc. Natl. Acad. Sci. U. S. A.* **112**, 1662–1629 (2015).
637 3. Visscher, P. M. *et al.* 10 years of GWAS discovery: Biology, function, and translation.
638 *Am. J. Hum. Genet.* **101**, 5–22 (2017).
639 4. Walsh, B. & Blows, M. W. Abundant Genetic Variation + Strong Selection =
640 Multivariate Genetic Constraints: A Geometric View of Adaptation. *Annu. Rev. Ecol.*
641 *Evol. Syst.* **40**, 41–59 (2009).
642 5. Johnston, S. E. *et al.* Life history trade-offs at a single locus maintain sexually selected
643 genetic variation. *Nature* **502**, 93–95 (2013).
644 6. Connallon, T. & Hall, M. D. Genetic constraints on adaptation: a theoretical primer for
645 the genomics era. *Ann. N. Y. Acad. Sci.* **1422**, 65–87 (2018).
646 7. Arnqvist, G. & Tuda, M. Sexual conflict and the gender load: Correlated evolution
647 between population fitness and sexual dimorphism in seed beetles. *Proc. R. Soc. B*
648 *Biol. Sci.* **277**, 1345–1352 (2010).
649 8. Whitlock, M. C. & Agrawal, A. F. Purging the genome with sexual selection:
650 Reducing mutation load through selection on males. *Evolution* **63**, 569–582 (2009).
651 9. Gilks, W. P., Abbott, J. K. & Morrow, E. H. Sex differences in disease genetics:
652 Evidence, evolution, and detection. *Trends Genet.* **30**, 453–463 (2014).
653 10. Kidwell, J. F., Clegg, M. T., Stewart, F. M. & Prout, T. Regions of stable equilibria for
654 models of differential selection in the two sexes under random mating. *Genetics* **85**,
655 171–183 (1977).
656 11. Curtsinger, J. W., Service, P. M. & Prout, T. Antagonistic pleiotropy, reversal of

657 dominance, and genetic polymorphism. *Am. Nat.* **144**, 210–228 (1994).
658 12. Charlesworth, B. & Charlesworth, D. A model for the evolution of fioecy and
659 gynodioecy. *Am. Nat.* **112**, 975–997 (1978).
660 13. Olito, C. & Connallon, T. Sexually antagonistic variation and the evolution of
661 dimorphic sexual systems. *Am. Nat.* **193**, 688–701 (2019).
662 14. Van Doorn, G. S. & Kirkpatrick, M. Turnover of sex chromosomes induced by sexual
663 conflict. *Nature* **449**, 909–912 (2007).
664 15. Charlesworth, D. & Charlesworth, B. Sex differences in fitness and selection for
665 centric fusions between sex-chromosomes and autosomes. *Genet. Res.* **35**, 205–214
666 (1980).
667 16. Jordan, C. Y. & Charlesworth, D. The potential for sexually antagonistic
668 polymorphism in different genome regions. *Evolution* **66**, 505–516 (2012).
669 17. Kirkpatrick, M. & Guerrero, R. F. Signatures of sex-antagonistic selection on
670 recombining sex chromosomes. *Genetics* **197**, 531–541 (2014).
671 18. Patten, M. M. & Haig, D. Maintenance or loss of genetic variation under sexual and
672 parental antagonism at a sex-linked locus. *Evolution* **63**, 2888–2895 (2009).
673 19. Bonduriansky, R. & Chenoweth, S. F. Intralocus sexual conflict. *Trends Ecol. Evol.*
674 **24**, 280–288 (2009).
675 20. Connallon, T. & Clark, A. G. Evolutionary inevitability of sexual antagonism. *Proc. R.*
676 *Soc. B Biol. Sci.* **281**, 2013–2123 (2014).
677 21. Cox, R. M. & Calsbeek, R. Sexually antagonistic selection, sexual dimorphism, and
678 the resolution of intralocus sexual conflict. *Am. Nat.* **173**, 176–187 (2009).
679 22. Singh, A. & Punzalan, D. The strength of sex-specific selection in the wild. *Evolution*
680 **72**, 2818–2824 (2018).
681 23. De Lisle, S. P., Goedert, D., Reedy, A. M. & Svensson, E. I. Climatic factors and

682 species range position predict sexually antagonistic selection across taxa. *Philos.*
683 *Trans. R. Soc. B Biol. Sci.* **373**, 20170415 (2018).
684 24. Mackay, T. F. C. The genetic architecture of quantitative traits. *Annu. Rev. Genet.* **35**,
685 303–339 (2001).
686 25. Delph, L. F. *et al.* Environment-dependent intralocus sexual conflict in a dioecious
687 plant. *New Phytol.* **192**, 542–552 (2011).
688 26. Svensson, E. I., McAdam, A. G. & Sinervo, B. Intralocus sexual conflict over immune
689 defense, gender load, and sex-specific signaling in a natural lizard population.
690 *Evolution* **63**, 3124–3135 (2009).
691 27. Chippindale, A. K., Gibson, J. R. & Rice, W. R. Negative genetic correlation for adult
692 fitness between sexes reveals ontogenetic conflict in *Drosophila*. *Proc. Natl. Acad.*
693 *Sci. U. S. A.* **98**, 1671–1675 (2001).
694 28. Stulp, G., Kuijper, B., Buunk, A. P., Pollet, T. V & Verhulst, S. Intralocus sexual
695 conflict over human height. *Biol. Lett.* **8**, 976–8 (2012).
696 29. Sanjak, J. S., Sidorenko, J., Robinson, M. R., Thornton, K. R. & Visscher, P. M.
697 Evidence of directional and stabilizing selection in contemporary humans. *Proc. Natl.*
698 *Acad. Sci. U. S. A.* **115**, 151–156 (2017).
699 30. Stearns, S. C., Govindaraju, D. R., Ewbank, D. & Byars, S. G. Constraints on the
700 coevolution of contemporary human males and females. *Proc. R. Soc. B Biol. Sci.* **279**,
701 4836–4844 (2012).
702 31. Ruzicka, F. *et al.* The search for sexually antagonistic genes: Practical insights from
703 studies of local adaptation and statistical genomics. *Evol. Lett.* **4**, 398–415 (2020).
704 32. Ruzicka, F. *et al.* Genome-wide sexually antagonistic variants reveal long-standing
705 constraints on sexual dimorphism in fruit flies. *PLoS Biol.* **17**, e3000244 (2019).
706 33. Cheng, C. & Kirkpatrick, M. Sex-specific selection and sex-biased gene expression in

707 humans and flies. *PLoS Genet.* **12**, e1006170 (2016).
708 34. Lucotte, E. A., Laurent, R., Heyer, E., Ségurel, L. & Toupance, B. Detection of allelic
709 frequency differences between the sexes in humans: a signature of sexually
710 antagonistic selection. *Genome Biol. Evol.* **8**, 1489–1500 (2016).
711 35. Wright, A. E. *et al.* Sex-biased gene expression resolves sexual conflict through the
712 evolution of sex-specific genetic architecture. *Evol. Lett.* **2**, 52–61 (2018).
713 36. Flanagan, S. P. & Jones, A. G. Genome-wide selection components analysis in a fish
714 with male pregnancy. *Evolution* **71**, 1096–1105 (2017).
715 37. Dutoit, L. *et al.* Sex-biased gene expression, sexual antagonism and levels of genetic
716 diversity in the collared flycatcher (*Ficedula albicollis*) genome. *Mol. Ecol.* **27**, 3572–
717 3581 (2018).
718 38. Bissegger, M., Laurentino, T. G., Roesti, M. & Berner, D. Widespread intersex
719 differentiation across the stickleback genome – The signature of sexually antagonistic
720 selection? *Mol. Ecol.* **29**, 262–271 (2019).
721 39. Mank, J. E., Shu, J. J. & Wright, A. E. Signature of sexual conflict is actually conflict
722 resolved. *Mol. Ecol.* (2020) doi:10.1111/mec.15311.
723 40. Cheng, C. & Kirkpatrick, M. The signal of sex-specific selection in humans is not an
724 artefact: Reply to Mank et al. *Mol. Ecol.* (2020) doi:10.1111/mec.15420.
725 41. Kasimatis, K. R. *et al.* Evaluating human autosomal loci for sexually antagonistic
726 viability selection in two large biobanks. *Genetics* **217**, 1–10 (2021).
727 42. Kasimatis, K. R., Ralph, P. L. & Phillips, P. C. Limits to genomic divergence under
728 sexually antagonistic selection. *G3* **9**, 3813–3824 (2019).
729 43. Mank, J. E. Population genetics of sexual conflict in the genomic era. *Nat. Rev. Genet.*
730 **18**, 721–730 (2017).
731 44. Rowe, L., Chenoweth, S. F. & Agrawal, A. F. The genomics of sexual conflict. *Am.*

732 *Nat.* **192**, 274–286 (2018).
733 45. Kasimatis, K. R., Nelson, T. C. & Phillips, P. C. Genomic signatures of sexual
734 conflict. *J. Hered.* **108**, 780–790 (2017).
735 46. Roberts, R. B., Ser, J. R. & Kocher, T. D. Sexual conflict resolved by invasion of a
736 novel sex determiner in Lake Malawi cichlid fishes. *Science* **326**, 998–1001 (2009).
737 47. Rostant, W. G., Kay, C., Wedell, N. & Hosken, D. J. Sexual conflict maintains
738 variation at an insecticide resistance locus. *BMC Biol.* **13**, 34 (2015).
739 48. Barson, N. J. *et al.* Sex-dependent dominance at a single locus maintains variation in
740 age at maturity in salmon. *Nature* **528**, 405–408 (2015).
741 49. VanKuren, N. W. & Long, M. Gene duplicates resolving sexual conflict rapidly
742 evolved essential gametogenesis functions. *Nat. Ecol. Evol.* **2**, 705–712 (2018).
743 50. Pearse, D. E. *et al.* Sex-dependent dominance maintains migration supergene in
744 rainbow trout. *Nat. Ecol. Evol.* **3**, 1731–1742 (2019).
745 51. Bycroft, C. *et al.* The UK Biobank resource with deep phenotyping and genomic data.
746 *Nature* (2018) doi:10.1038/s41586-018-0579-z.
747 52. Wright, S. The genetical structure of species. *Ann. Eugen.* **15**, 323–354 (1951).
748 53. Eyre-Walker, A. Genetic architecture of a complex trait and its implications for fitness
749 and genome-wide association studies. *Proc. Natl. Acad. Sci. U. S. A.* **107**, 1752–1756
750 (2010).
751 54. Pirastu, N. *et al.* Genetic analyses identify widespread sex-differential participation
752 bias. *bioRxiv* (2020).
753 55. Albers, P. K. & McVean, G. Dating genomic variants and shared ancestry in
754 population-scale sequencing data. *PLoS Biol.* **18**, (2020).
755 56. The 1000 Genomes Project Consortium. A global reference for human genetic
756 variation. *Nature* **526**, 68–74 (2015).

757 57. Andrés, A. M. *et al.* Targets of balancing selection in the human genome. *Mol. Biol.*
758 *Evol.* **26**, 2755–2764 (2009).
759 58. Bitarello, B. D. *et al.* Signatures of long-term balancing selection in human genomes.
760 *Genome Biol. Evol.* **10**, 939–955 (2018).
761 59. DeGiorgio, M., Lohmueller, K. E. & Nielsen, R. A model-based approach for
762 identifying signatures of ancient balancing selection in genetic data. *PLoS Genet.* **10**,
763 e1004561 (2014).
764 60. Morrissey, M. B. Meta-analysis of magnitudes, differences and variation in
765 evolutionary parameters. *J. Evol. Biol.* **29**, 1882–1904 (2016).
766 61. Vitti, J. J., Grossman, S. R. & Sabeti, P. C. Detecting natural selection in genomic
767 data. *Annu. Rev. Genet* **47**, 97–120 (2013).
768 62. Hoban, S. *et al.* Finding the genomic basis of local adaptation: Pitfalls, practical
769 solutions, and future directions. *Am. Nat.* **188**, 379–397 (2016).
770 63. Booker, T. R., Jackson, B. C. & Keightley, P. D. Detecting positive selection in the
771 genome. *BMC Biol.* **15**, (2017).
772 64. Stearns, S. C., Byars, S. G., Govindaraju, D. R. & Ewbank, D. Measuring selection in
773 contemporary human populations. *Nat. Rev. Genet.* **11**, 611–622 (2010).
774 65. Bernabeu, E. *et al.* Sex differences in genetic architecture in UK Biobank. *Nat. Genet.*
775 **53**, 1283–1289 (2021).
776 66. Benagiano, G., Farris, M. & Grudzinskas, G. Fate of fertilized human oocytes. *Reprod.*
777 *Biomed. Online* **21**, 732–741 (2010).
778 67. Lucotte, E. A. *et al.* Detection of sexually antagonistic transmission distortions in trio
779 datasets. *bioRxiv* (2020) doi:10.1101/2020.09.11.293191.
780 68. http://www.nealelab.is/uk-biobank/.
781 69. Fijarczyk, A. & Babik, W. Detecting balancing selection in genomes: Limits and

782 prospects. *Mol. Ecol.* **24**, 3529–3545 (2015).
783 70. Li, H. & Durbin, R. Inference of human population history from individual whole-
784 genome sequences. *Nature* **475**, 493–496 (2011).
785 71. Connallon, T. & Clark, A. G. A general population genetic framework for antagonistic
786 selection that accounts for demography and recurrent mutation. *Genetics* **190**, 1477–
787 1489 (2012).
788 72. Connallon, T. & Clark, A. G. Antagonistic versus nonantagonistic models of balancing
789 selection: characterizing the relative timescales and hitchhiking effects of partial
790 selective sweeps. *Evolution* **67**, 908–917 (2013).
791 73. Janicke, T., Häderer, I. K., Lajeunesse, M. J. & Anthes, N. Darwinian sex roles
792 confirmed across the animal kingdom. *Sci. Adv.* **2**, e1500983 (2016).
793 74. Eyre-Walker, A. & Keightley, P. D. The distribution of fitness effects of new
794 mutations. *Nat. Rev. Genet.* **8**, 610–618 (2007).
795 75. Yeaman, S. Local adaptation by alleles of small effect. *Am. Nat.* **186**, S74–S89 (2015).
796 76. Connallon, T., Débarre, F. & Li, X. Y. Linking local adaptation with the evolution of
797 sex differences. *Philos. Trans. R. Soc. B Biol. Sci.* **373**, 20170414 (2018).
798 77. Mullon, C., Pomiankowski, A. & Reuter, M. The effects of selection and genetic drift
799 on the genomic distribution of sexually antagonistic alleles. *Evolution* **66**, 3743–3753
800 (2012).
801 78. Chang, C. C. *et al.* Second-generation PLINK: Rising to the challenge of larger and
802 richer datasets. *Gigascience* **4**, (2015).
803 79. Benjamini, Y. & Hochberg, Y. Controlling the false discovery rate: a practical and
804 powerful approach to multiple testing. *J. R. Stat. Soc.* **57**, 289–300 (1995).
805 80. Zietsch, B. P., Kuja-Halkola, R., Walum, H. & Verweij, K. J. H. Perfect genetic
806 correlation between number of offspring and grandoffspring in an industrialized

807 human population. *Proc. Natl. Acad. Sci. U. S. A.* **111**, 1032–1036 (2014).
808 81. Loh, P.-R., Kichaev, G., Gazal, S., Schoech, A. & Price, A. Mixed model association
809 for biobank-scale data sets. *Nat. Genet.* **50**, 906–908 (2018).
810 82. Randall, J. C. *et al.* Sex-stratified genome-wide association studies including 270,000
811 individuals show sexual dimorphism in genetic loci for anthropometric traits. *PLoS*
812 *Genet.* **9**, e1003500 (2013).
813 83. Coop, G. *et al.* The role of geography in human adaptation. *PLoS Genet.* **5**, e1000500.
814 (2009).
815 84. Barreiro, L. B., Laval, G., Quach, H., Patin, E. & Quintana-Murci, L. Natural selection
816 has driven population differentiation in modern humans. *Nat. Genet.* **40**, 340–345
817 (2008).
818 85. Key, F. M., Fu, Q., Romagne, F., Lachmann, M. & Andres, A. M. Human adaptation
819 and population differentiation in the light of ancient genomes. *Nat. Commun.* **7**, 10775
820 (2016).
821 86. Cingolani, P. *et al.* A program for annotating and predicting the effects of single
822 nucleotide polymorphisms, SnpEff. *Fly (Austin).* **6**, 80–92 (2012).
823 87. Connallon, T., Sharma, S. & Olito, C. Evolutionary consequences of sex-specific
824 selection in variable environments: Four simple models reveal diverse evolutionary
825 outcomes. *Am. Nat.* **193**, 93–105 (2019).
826 88. Crow, J. F. & Kimura, M. *An Introduction to Population Genetics Theory*. (Harper and
827 Row, 1970). doi:10.2307/1529706.
828 89. Smith, S. R. T. & Connallon, T. The contribution of the mitochondrial genome to sex-
829 specific fitness variance. *Evolution* **71**, 1417–1424 (2017).
830 90. Morrow, E. H. & Connallon, T. Implications of sex-specific selection for the genetic
831 basis of disease. *Evol. Appl.* **6**, 1208–1217 (2013).

91. Connallon, T. & Jordan, C. Y. Accumulation of deleterious mutations near sexually antagonistic genes. *G3* **6**, 2273–84 (2016).

## Acknowledgements

We thank Tom Allison, Isobel Beasley, Isobel Booksmythe, Katja Kasimatis and three anonymous reviewers for helpful comments on previous versions of the manuscript. This work was supported by the Monash Bioinformatics Platform, the UK Biobank (project number 52049 to FR and TC), and funds from the Australian Research Council (to TC).

## Author contributions

Conceptualization: FR, LH, TC; Methodology: FR, LH, TC; Investigation: FR, LH, TC; Visualization: FR, LH, TC; Funding acquisition: TC; Project administration: FR, TC; Supervision: FR, LH, TC; Writing – original draft: FR, TC; Writing – review & editing: FR, LH, TC.

## Competing Interests

Authors declare no competing interests.

## Data accessibility

Within the restrictions of the UK Biobank MTA agreement, metadata will be made available in the Supplementary Materials. Further metadata will be made available on public data sharing platforms, and code will be made available on public github repositories upon publication (/filruzicka/polygenic_SA_selection_in_the_UK_biobank/ and /lukeholman/ukbb_sex_fst/).

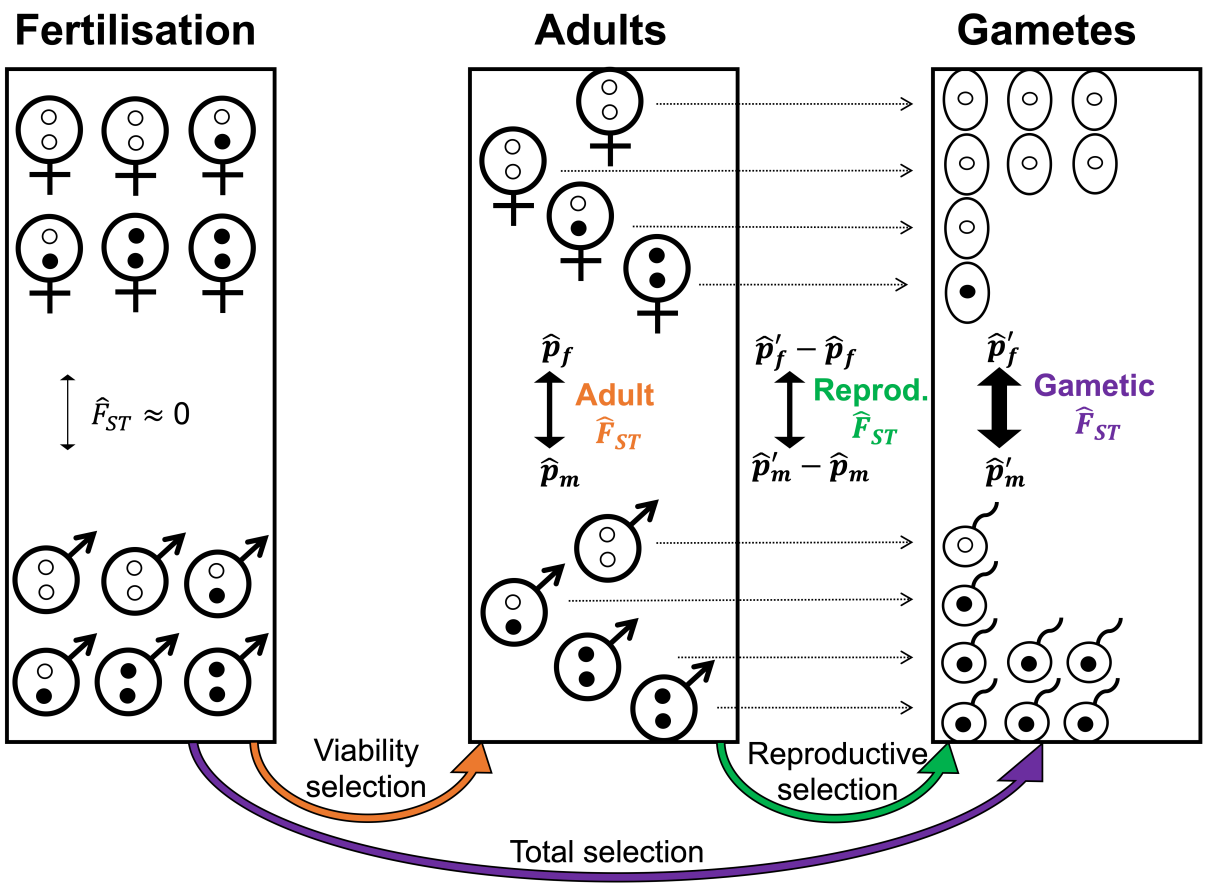


**Figure 1. Partitioning signals of sex differences in selection among fitness components.** A pair of autosomal alleles at a locus are represented by black and white dots, representing male-beneficial and female-beneficial alleles, respectively; $\hat{p}_f$, $\hat{p}_m$, $\hat{p}'_f$, and $\hat{p}'_m$ depict sex-specific frequency estimates for a given allele at different stages of the life cycle (see main text for details). Autosomal allele frequencies are equalised between sexes at fertilisation (left box; females, top; males, bottom), resulting in negligible allele frequency differentiation at this stage of the life cycle. Differentiation between sexes can arise in the sample of adults (middle box) due to sex differences in viability selection among juveniles (orange arrow), and in the projected gametes (right box) due to sex differences in lifetime reproductive success (LRS) among adults (green arrow). Data on sex-specific allele frequencies and LRS thus allow the estimation of sex-differential effects of genetic variants on each fitness component (including overall fitness; purple arrow), despite the absence of allele frequency data among zygotes (left box) and gametes (right box), which are inferred and not directly observed.

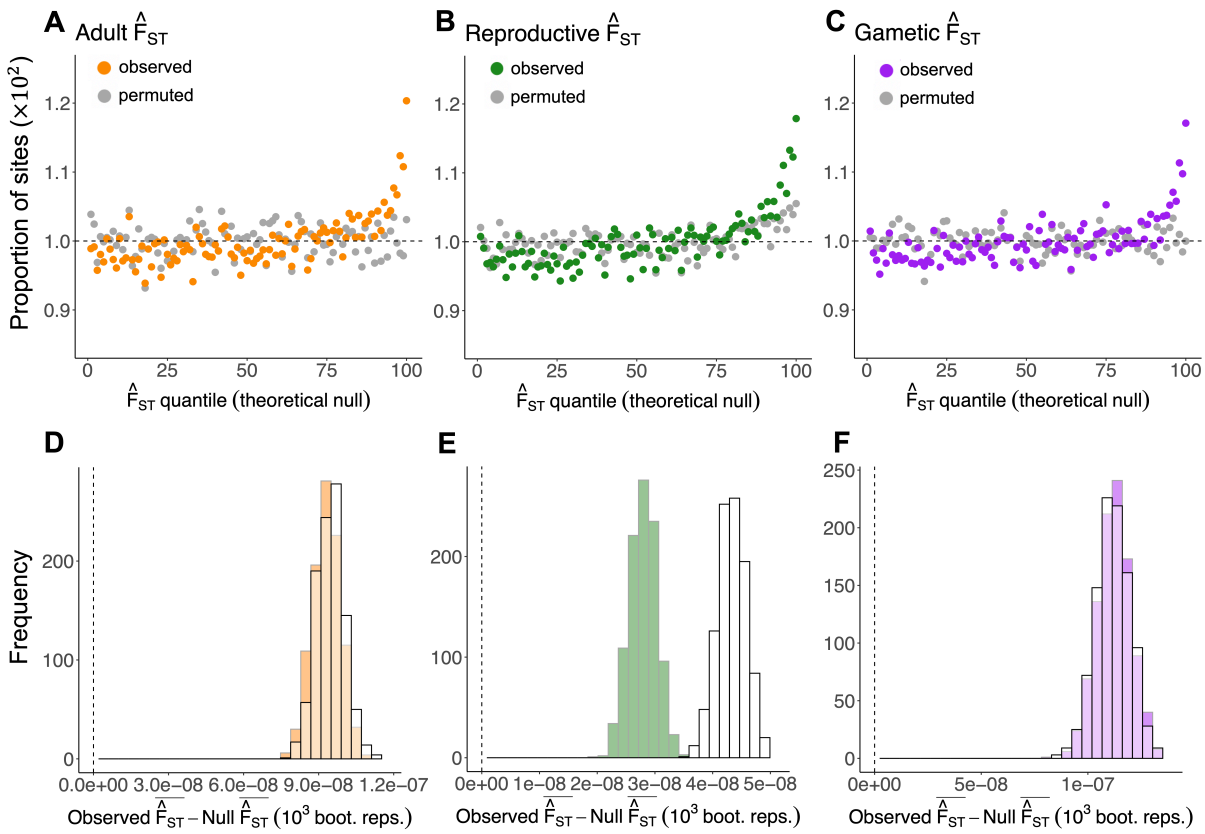


**Figure 2. Polygenic signals of SA selection: inflation in $\hat{F}_{ST}$ metrics relative to their nulls.** **A-C**. Proportion of sites (coloured, observed; grey, permuted) falling into each of 100 quantiles of the theoretical null distributions of adult $\hat{F}_{ST}$ (A), reproductive $\hat{F}_{ST}$ (B) and gametic $\hat{F}_{ST}$ (C). Theoretical null data (*x*-axes) were generated by simulating $\hat{F}_{ST}$ values (nSNPs = 544,635) from the relevant theoretical null distributions (*i.e.*, eqs. [3a-c] for adult, reproductive and gametic $\hat{F}_{ST}$, respectively). In the absence of sex differences in selection, approximately 1% of SNPs should fall into each quantile of the relevant theoretical null (dashed line). **D-F.** Difference between the mean of each metric (adult, reproductive and gametic $\hat{F}_{ST}$, respectively) in observed and empirical null data (coloured histograms) and in observed and theoretical null data (white histograms), across 1,000 bootstrap replicates. Vertical line intersects zero (no difference between observed and null data). Differences are greater than zero across comparisons and metrics for all bootstrap replicates, so all p-values are p<0.001.

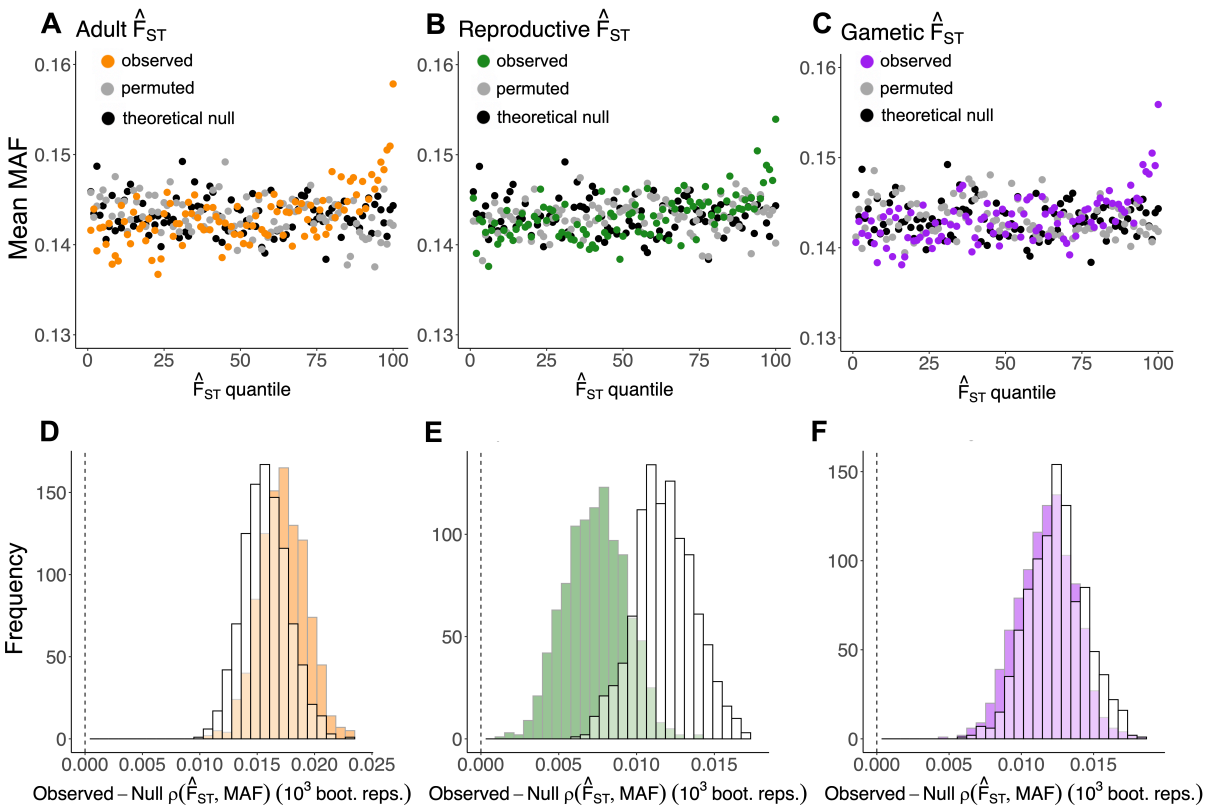


885

886 **Figure 3. Polygenic signals of SA selection: positive associations between $\hat{F}_{ST}$ metrics and**

887 **MAF. A-C**. Mean MAF (coloured, observed; grey, permuted; black, theoretical) among 100

888 quantiles of adult $\hat{F}_{ST}$ (D), reproductive $\hat{F}_{ST}$ (E) and gametic $\hat{F}_{ST}$ (F). Quantiles for theoretical

889 null data were obtained as in Fig. 2A-C; quantiles for observed and permuted data were

890 obtained from observed and permuted $\hat{F}_{ST}$ distributions for each respective metric. **D-F.**

891 Difference between the Spearman's rank correlation in the observed and empirical null data

892 (coloured histograms) and between observed and theoretical null data (white histograms),

893 across 1,000 bootstrap replicates, where the correlation is between each $\hat{F}_{ST}$ metric (adult,

894 reproductive and gametic $\hat{F}_{ST}$, respectively) and MAF. Vertical line intersects zero (no

895 difference between observed and null data). Differences are greater than zero across

896 comparisons and metrics for all bootstrap replicates, so all p-values are $p<0.001$.

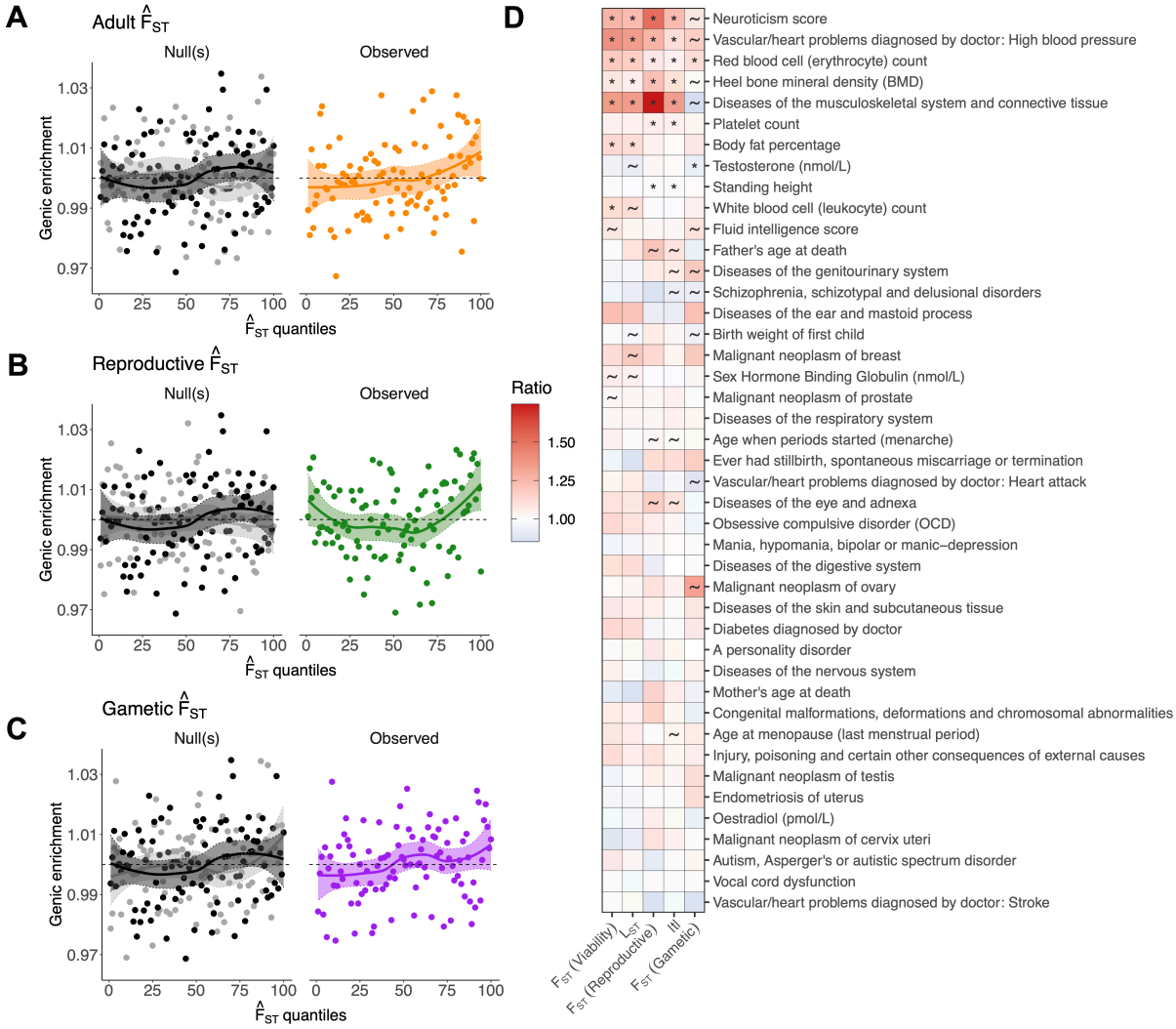


**Figure 4. Candidate SA polymorphisms are more likely to be functional and contribute to trait variation. A-C.** Genic enrichment (coloured, observed; grey, permuted; black, theoretical) in each of 100 quantiles of adult $\hat{F}_{ST}$ (A), reproductive $\hat{F}_{ST}$ (B) and gametic $\hat{F}_{ST}$ (C). Quantiles for theoretical null data, permuted data and observed data were obtained as in Fig. 3A-C. Genic enrichment is defined as the proportion of sites in a given quantile that are genic divided by the proportion of all sites that are genic. Loess curves (±SE) are presented for visual emphasis. **D.** Relationships between five metrics of sex-differential selection and candidate loci for various UK Biobank phenotypes (as analysed by the Neale laboratory), using an LD-pruned set of imputed SNPs. Each tile compares the mean value of the relevant metric of sex-differential selection between variants that are associated and not associated with the

focal phenotype, with colours denoting the ratio of means (with ratios >1 indicating *e.g.* higher $\hat{F}_{ST}$ among associated than non-associated variants), and statistical significance assessed using a Mann-Whitney test (*, FDR-adjusted p<0.05; ~, unadjusted p<0.05).

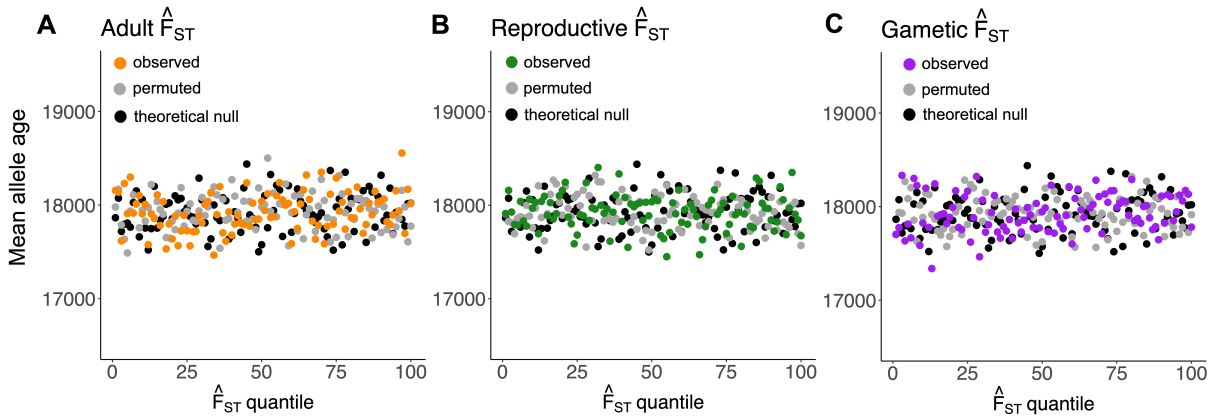


**Figure 5. No evidence that candidate SA polymorphisms are older than average.** Mean age of the alternative (*i.e.*, non-reference) allele (coloured, observed; grey, permuted; black, theoretical) across 100 quantiles of adult $\hat{F}_{ST}$ (A), reproductive $\hat{F}_{ST}$ (B) and gametic $\hat{F}_{ST}$ (C). Quantiles for theoretical null data, permuted data and observed data were obtained as in Fig. 3A-C. All panels correct for ascertainment bias of alternative allele frequencies. For visualisation purposes, this was done by averaging, in each $\hat{F}_{ST}$ quantile, mean allele age across 20 quantiles of alternative allele frequency in the UK Biobank (such that alternative allele frequency is approximately equal across $\hat{F}_{ST}$ quantiles).